# Intramolecular dynamic nuclear polarization via electron-nuclear double resonance

A. S. Brill
*Department of Physics, University of Virginia, Charlottesville, Virginia 22904-4714*
(Received 29 April 2002; published 7 October 2002)

A fast and low power method is proposed and simulated for achieving substantial intramolecular dynamic nuclear polarization, as high as 50% for protons and 17% for deuterons, by means of simultaneous nuclear and allowed electronic magnetic resonance transitions.

DOI: 10.1103/PhysRevA.66.043405 PACS number(s): 33.25.+k, 33.35.+r, 33.40.+f

## I. INTRODUCTION

Because electronic magnetic moments are orders of magnitude greater than nuclear magnetic moments, for a given magnetic field strength and temperature, the polarization of electron spins far exceeds that of nuclear spins. However, strong nuclear spin polarization is often an important experimental condition. For example, the sensitivities of many kinds of measurement depend upon the extent of such polarization (see e.g., [1–3]), and nuclear fusion rates are affected by polarization of the reacting nuclei [4]. Dynamic nuclear polarization (DNP) processes enable experimenters to transfer electron spin polarization to nuclear spin systems [5]. Among its applications, DNP is employed to polarize targets for experiments on spin-dependent scattering by fundamental particles [6], to increase the contrast in polarized neutron small-angle scattering from frozen spin targets of biological origin [7], and to increase magnetic resonance signals, e.g., [7,8]. In this paper a method, combining electron-nuclear double resonance and DNP, (ENDOR-DNP) is proposed for achieving as high as 50% polarization of protons and 17% of deuterons in far less time and with much lower microwave power than present DNP methods. As currently used, DNP depends upon forbidden electron paramagnetic resonance (EPR) transitions in a target containing a low concentration of paramagnetic centers (e.g., $NH_2$ free radicals) each surrounded by a ''sea'' of polarizable nuclei (e.g., protons in frozen ammonia); here electron spin–nuclear spin magnetic dipole interactions give rise to the nuclear spin-state mixing (small in amount) responsible for the forbidden transitions. The possibility of producing a significantly greater amount of spin-state mixing, or interchange, in the excited electronic state by electron-nuclear double resonance [9] has apparently been overlooked. Application of ENDOR would require, in addition to the microwave field already dedicated to exciting EPR transitions, a radio frequency magnetic field (with both the microwave and rf fields polarized perpendicular to the large steady magnetic field). Because of hyperfine interactions and the nuclear Zeeman effect acting together, separations in energy between ''adjacent'' (i.e., $\Delta m_I=1$) nuclear spin states of the excited electronic manifold differ from those of the ground electronic manifold (as in $NH_2$ and $ND_2$, [10]); these differences in splitting ensure that the rf field (employed to mix states within the excited manifold) will not induce depolarizing transitions within the ground manifold. For $I>1/2$, quadrupole hyperfine shifts make the splittings between adjacent pairs of each electronic manifold different.

## II. ENERGY LEVELS

A hyperfine-coupled system consisting of a single electron spin (distant from other electron spins) and an $I=1/2$ nuclear spin (the $I=1$ case to be discussed later) in the presence of three applied magnetic fields is treated. One of the fields, $B$, is constant; one, $B_{rf}$, is at the radio frequency ($\omega_{rf}$) for the NMR transition between nuclear levels of the excited electronic state; and one, $B_{\mu w}$, is at a microwave frequency ($\omega_{\mu w}$) for one of the allowed EPR transitions. The electronic $g$ tensor is taken to be close to isotropic so that the spread in the EPR transitions associated with random orientation of the sites is much narrower than the hyperfine splittings (also taken essentially isotropic). Figure 1 shows, schematically, the dependence of energy levels upon the strength of the steady magnetic field $B$. The ordering in energy of $a$ and $b$, the nuclear levels in the ground electronic state ($m_s=-1/2$), is for the proton with $B>B_{cross}$, where $B_{cross}$ is the applied field at which these levels are closest together (e.g., about 0.6 T in $NH_2$) [10]. The ordering of $c$ and $d$, the nuclear levels in the excited electronic state ($m_s=+1/2$), for the proton, is independent of $B$. In Fig. 1 the relative energies of the electronic Zeeman splitting ($0.93\ \mathrm{cm}^{-1}\ \mathrm{T}^{-1}$ for $g_{electronic}=2.0$) and the joint hyperfine-nuclear Zeeman splittings (of the order of $10^{-3}\ \mathrm{cm}^{-1}$ in free radicals) are unrealistic; for $B>B_{cross}$ the former energy greatly exceeds the latter. The $\varepsilon$'s are coefficients of nuclear spin-state mixing; for example, $|\varepsilon_{gnd}|^2$ is the population ratio of $m_I=-1/2$ to $m_I=+1/2$ in level a and of $m_I=+1/2$ to $m_I=-1/2$ in level $b$. $N_{gnd}=(1+|\varepsilon_{gnd}|^2)^{-1/2}$ is the normalization coefficient for both $a$ and $b$. For large $B$, which is a favorable experimental condition for the method explored here, $|\varepsilon|^2$ is small and approximates the fractional population of the minor nuclear spin-state constituent.

The symbols $f_a$, $f_b$, $f_c$, and $f_d$ will be used to designate the fractional populations of the states such that $f_a+f_b+f_c+f_d=1$. At temperature $T$, with $k_B$ the Boltzmann constant, the thermal equilibrium values are $f_{b,eq}/f_{a,eq}=\exp[-(E_b-E_a)/k_BT]$, $f_{c,eq}/f_{a,eq}=\exp[-(E_c-E_a)/k_BT]$, $f_{d,eq}/f_{a,eq}=\exp[-(E_d-E_a)/k_BT]$, and $f_{a,eq}=1/(1+f_{b,eq}/f_{a,eq}+f_{c,eq}/f_{a,eq}+f_{d,eq}/f_{a,eq})$. At $T\approx 1$ K, $f_{a,eq}\approx f_{b,eq}\approx 0.5$, and $f_{c,eq}\approx f_{d,eq}\approx 0$.

In Fig. 1, the levels are shown as nuclear spin-state mixed. Such mixing is treated in detail in [10]. Overlap of the nuclear parts of the ground with the excited states affects transition and relaxation rates. In the exposition below, the overlap between levels $a$ and $d$ and between $b$ and $c$ is char-

 

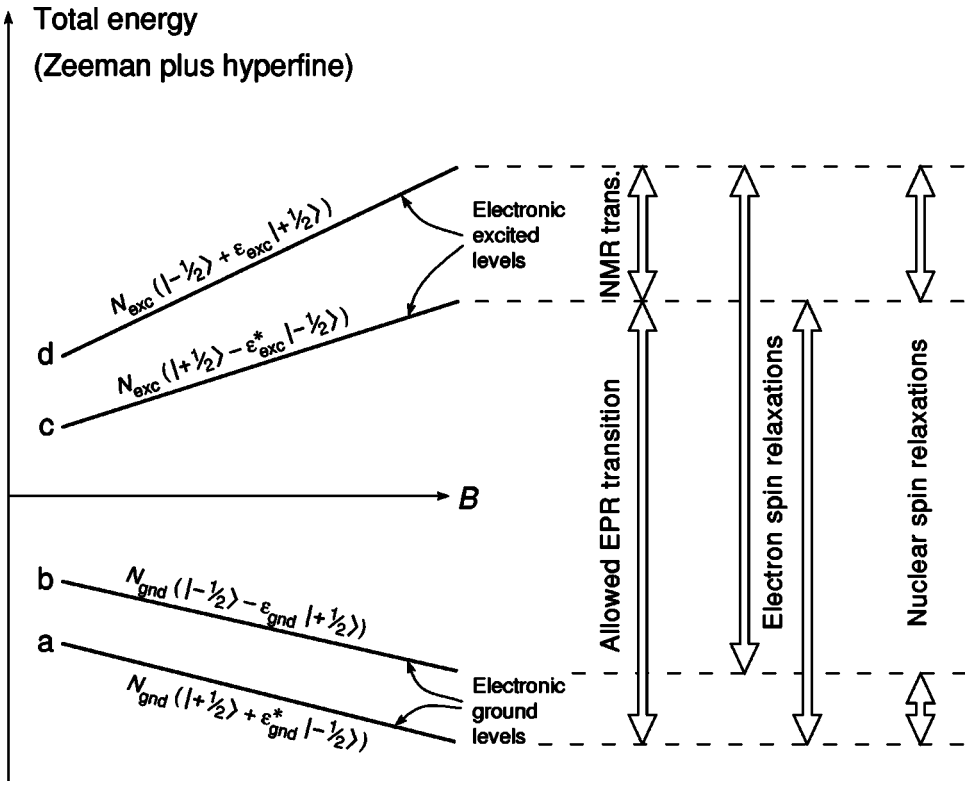


FIG. 1. Schematic example of the four energy levels of a hyperfine-coupled system, consisting of a single electron spin and an $I=1/2$ nuclear spin, as a function of the strength of an applied magnetic field $B$. Each of the four levels is a nuclear spin-state mixture of $|m_I=-1/2\rangle$ and $|m_I=+1/2\rangle$, as shown, where the $\varepsilon$'s are the mixing parameters and the $N$'s are nomalization coefficients. As $B$ and the nuclear Zeeman interaction increase, the $\varepsilon$'s $\rightarrow 0$ and the $N's \rightarrow 1$. The pair of lower electronic Zeeman energy (the ground levels) has $m_s=-1/2$ and the pair of higher electronic Zeeman energy (the excited levels) has $m_s=+1/2$. The ordering in energy depicted within the pairs is taken to be that for a proton in $NH_2$ subject to $B>B_{cross}$ [10].

acterized by the parameter $\lambda^2$ $(=\lambda_{ad}^2=\lambda_{bc}^2)$, as defined for levels $a$ and $d$ by

$$\lambda_{ad}^2 \equiv |\langle a_{nuclear}|d_{nuclear}\rangle|^2$$

with

$$|a_{nuclear}\rangle \quad \text{and} \quad |d_{nuclear}\rangle \ \text{normalized}$$

and analogously for states $b$ and $c$. For the system of Fig. 1

$$\begin{aligned}\lambda_{ac}^2 &\equiv |\langle a_{nuclear}|c_{nuclear}\rangle|^2 = |\langle b_{nuclear}|d_{nuclear}\rangle|^2 \\ &\equiv \lambda_{bd}^2 \\ &= 1-\lambda^2.\end{aligned}$$

As $B$ increases beyond $B_{cross}$, nuclear Zeeman interaction becomes the dominant factor in nuclear spin quantization so that nuclear spin-state mixing $(|\varepsilon|^2)$ diminishes monotonically, and the $ac$ and $bd$ overlaps approach 1. For large $B$, e.g., protons in $NH_2$ at $B=5$ T, $\lambda^2$ is too small to have a noticeable effect on the processes to be treated here.

### III. RATE EQUATIONS

Also indicated in Fig. 1 are four kinds of rate process. The rate constants for the four intramolecular processes are $k_E$ and $k_N$, the EPR and NMR transition probabilities; $r_E$, the electron spin-lattice relaxation rate; and $r_N$, the nuclear spin-lattice relaxation rate, which can be different for nuclear spins in the ground and excited electronic states. Which allowed EPR transition is chosen is determined by the polarization sought; the $a$ to $c$ transition shown in this figure produces down-field, i.e., negative, polarization. The four kinds of intramolecular process for nuclear spin 1/2 appear in the following rate equations, all first order and linear, for states $a$, $b$, and $c$:

$$\begin{aligned}df_a/dt = {} & k_E(1-\lambda^2)(f_c-f_a)+r_E[f_{a,eq}-f_a \\ & +(1-\lambda^2)(f_c-f_{c,eq})+\lambda^2(f_d-f_{d,eq})] \\ & +r_{N,gnd}(f_{a,eq}-f_a+f_b-f_{b,eq}),\end{aligned} \tag{1}$$

$$\begin{aligned}df_b/dt = {} & r_E[f_{b,eq}-f_b+\lambda^2(f_c-f_{c,eq}) \\ & +(1-\lambda^2)(f_d-f_{d,eq})]+r_{N,gnd}(f_a-f_{a,eq} \\ & +f_{b,eq}-f_b),\end{aligned} \tag{2}$$

$$\begin{aligned}df_c/dt = {} & k_E(1-\lambda^2)(f_a-f_c)+k_N(f_d-f_c) \\ & +r_E[(1-\lambda^2)(f_a-f_{a,eq})+\lambda^2(f_b-f_{b,eq}+f_{c,eq} \\ & -f_c]+r_{N,exc}(f_{c,eq}-f_c+f_{d,eq}-f_d).\end{aligned} \tag{3}$$

Because $f_a+f_b+f_c+f_d=1$, $df_d/dt=-(df_a/dt+df_b/dt+df_c/dt)$, i.e., the rate equation for $f_d$ is not independent of the set of equations (1), (2), and (3).

There is a fifth process, spin diffusion, which is responsible for the propagation of intramolecular nuclear polarization into the surrounding medium. The rate of spin diffusion depends upon the difference between intramolecular and neighboring polarization; because of the local magnetic field ''barrier'' from the unpaired electron magnetic dipole [11], this rate is slower than the nuclear spin relaxation rate in the distant medium. Spin diffusion begins to be effective after intramolecular polarization has developed; even after the

steady state is reached, spin diffusion has little effect upon, and will not be included with, the rate processes active in Eqs. (1)–(3) above. Nor does the surrounding medium, which is taken to have a low concentration of unpaired electron spins, affect the internal electron spin. Apart from the applied magnetic fields and the ''lattice'' (constant temperature bath) interactions responsible for electron and nuclear spin relaxation, the molecule treated here is isolated.

The polarization from a static field is up (i.e., in the direction of the field) if the nuclear $g$ value is positive and down for a negative $g$ value. With dynamic nuclear polarization, one can choose to polarize up or down. If the latter is chosen, Eqs. (1)–(3) apply and result in population changes in all four states, the largest in $a$ (a decrease) with smaller changes in the others (all increases). In more detail, but simplified with $\lambda^2 \approx 0$, one seeks to maximize the net fractional polarization

$$p = -(f_b + f_d - f_a - f_c). \tag{4}$$

When the energy of the microwave photons is equal to the energy difference between states $a$ and $c$, there are allowed EPR transitions between these states, and the $a$ to $c$ transition starts the polarization sequence. Because the transition is allowed, high microwave power is not required. In the absence of power saturation, the net EPR transition rate is $k_E(1-\lambda^2)(f_a - f_c)$, the negative of which is the first term in Eq. (1) above. Analogous to $k_E$ is $k_N$, in Eq. (3) above, the NMR transition probability. $r_E$ and $r_N$ characterize unmixed states, and so $\lambda^2$ and $1-\lambda^2$ are included to allow for the effects of nuclear spin-state mixing.

The following five rate equations are for nuclear spin 1. The case treated is a deuteron with $B > B_{cross}$. The levels are in order of increasing energy from $a$ to $e$. Quadrupole interaction makes $E_c - E_b > E_b - E_a$ and $E_f - E_e > E_e - E_d$. Down polarization is chosen, which requires states e and f to be connected by the NMR rf field.

$$df_a/dt = r_E[f_{a,eq} - fa + \lambda_{ad}^2(f_a - f_{a,eq}) + \lambda_{ae}^2(f_e - f_{e,eq}) + \lambda_{af}^2(f_f - f_{f,eq}] + r_{N,gnd}(f_{a,eq} - f_a + f_b - f_{b,eq}), \tag{5}$$

$$df_b/dt = -k_E\lambda_{be}^2(f_b - f_e) + r_E[f_{b,eq} - f_b + \lambda_{bd}^2(f_d - f_{d,eq}) + \lambda_{be}^2(f_e - f_{e,eq} + \lambda_{bf}^2(f_f - f_{f,eq})] + r_{N,gnd}[f_a - f_{a,eq} + 2(f_{b,eq} - f_b) + f_c - f_{c,eq}], \tag{6}$$

$$df_c/dt = r_E[f_{c,eq} - f_c + \lambda_{cd}^2(f_d - f_{d,eq}) + \lambda_{ce}^2(f_e - f_{e,eq}) + \lambda_{cf}^2(f_f - f_{f,eq}] + r_{N,gnd}(f_{b,eq} - f_b + f_c - f_{c,eq}), \tag{7}$$

$$df_d/dt = r_E[f_{d,eq} - f_d + \lambda_{ad}^2(f_a - f_{a,eq}) + \lambda_{bd}^2(f_b - f_{b,eq}) + \lambda_{cd}^2(f_c - f_{c,eq}] + r_{N,exc}(f_{d,eq} - f_d + f_e - f_{e,eq}) \tag{8}$$

$$df_e/dt = k_E\lambda_{be}^2(f_b - f_e) - k_N(f_e - f_f) + r_E[f_{e,eq} - f_e + \lambda_{ae}^2(f_a - f_{a,eq}) + \lambda_{be}^2(f_b - f_{b,eq}) + \lambda_{ce}^2(f_c - f_{c,eq})] + r_{N,exc}[f_d - f_{d,eq} + 2(f_{e,eq-fe}) + f_f - f_{f,eq}]. \tag{9}$$

Because $f_a + f_b + f_c + f_d + f_e + f_f = 1$, $df_f/dt$ is not independent of Eqs. (5)–(9).

## IV. RATE PARAMETERS

The rate equations (1)–(3) can be solved to obtain the time courses and steady-state values of the fractional populations $f_a$, $f_b$, $f_c$, and $f_d$, and Eqs. (5)–(9) solved for $f_a$ through $f_f$. For this purpose, realistic values of $k_E$, $k_N$, $r_E$, $r_{N,gnd}$, and $r_{N,exc}$ are required.

In order to be able to treat the kinetics of any DNP method quantitatively, it is necessary to know $r_E(T,B)$. However, apart from indirect estimates of $F$-center relaxation times in irradiated LiH [12], measurements of $r_E$ at the low temperatures and strong fields treated in the present exposition have not been reported. There is useful literature on the temperature dependence of $r_E$ for free radicals in magnetic fields of about 0.36 T. For this field and in the temperature range 5–20 K, $r_E$ for methyl radicals trapped in various matrices is proportional to the absolute temperature, with the constant of proportionality in the range 34 to 121 $K^{-1}$ $s^{-1}$ [13]. In a recent study, the relaxation rate of the nitroxide free radical tempol, doped into a diamagnetic host, was found to be the same at fields of 0.34 and 3.4 T between 50 and 250 K, a temperature range in which the rate is closely proportional to $T^2$ [14]. From 50 to 14 K, where data taken only at $B = 0.34$ T are presented in [14], the dependence of $r_E$ upon $T$ decreases with decreasing $T$; at 14 K, $r_E = 126$ $s^{-1}$. A 1 mM solution of another nitroxide free radical, 4-amino TEMPO (4-amino-2,2,6,6,-tetramethylpiperdine-1-oxyl), dissolved in a 60:40 glycerol/water solution, has $r_E \approx 13$ $s^{-1}$ at $T = 10$ K and $B = 5$ T [15]. In Ref. [6] the relaxation time of electron spins in irradiated ammonia at 1 K and 5 T is said to be ''short ($\approx 10^{-3}$ s),'' but the source of this information is not mentioned. In order to demonstrate the kinetic and steady-state behavior of ENDOR-DNP in the absence of tighter constraints upon $r_E$, the latter rate parameter will be given values of 1, 200, and 1000 $s^{-1}$ in the exposition below.

The contribution of paramagnetic ''impurities'' to the relaxation rate of nuclear spins in solids is well understood in its application to systems where the operative dipolar interaction is between electron and nuclear spins that are distant from each other [16]. In the case at hand, however, the electron spin and nuclear spin are in the same molecule. The off-diagonal operator for the distant dipolar coupling employed in the formulation of extramolecular spin-lattice relaxation [16] is replaced by $H_{mix}$, Eq. (2) of [10], the corresponding off-diagonal part of the intramolecular electron dipole–nuclear dipole Hamiltonian. The resulting expressions are

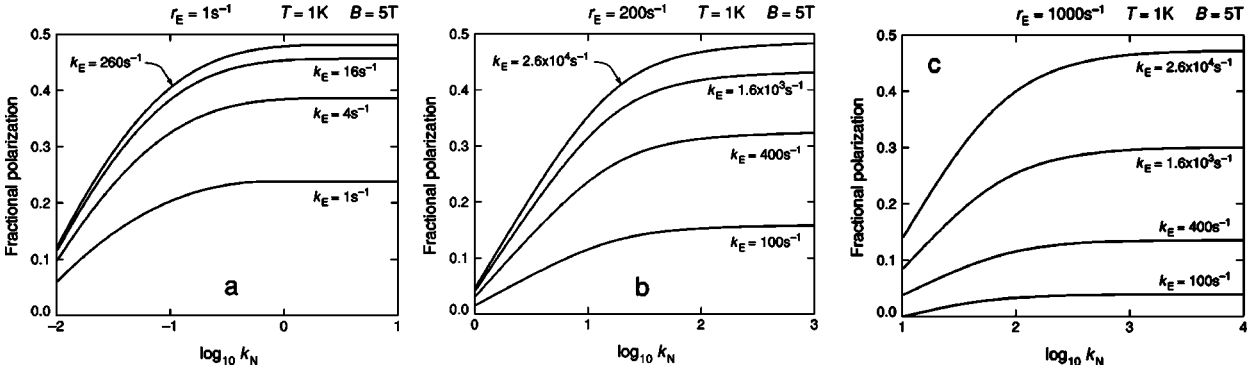


FIG. 2. Polarization of a proton in $NH_2$ as a function of $k_N$ for several values of $k_E$ when (a) $r_E = 1\ s^{-1}$, (b) $r_E = 200\ s^{-1}$, (c) $r_E = 1000\ s^{-1}$. $T = 1$ K and $B = 5$ T.

$$r_N = (8/3) r_E |H_{mix}|^2/(\hbar\omega_N)^2 \quad \text{for } I_N = 1/2 \tag{10a}$$

$$\text{and} \quad r_N = (4/3) r_E |H_{mix}|^2/(\hbar\omega_N)^2 \quad \text{for } I_N = 1. \tag{10b}$$

Here, $\omega_N$ is the frequency for a NMR transition between adjacent nuclear levels of either the ground or excited electronic state. For example, in $NH_2$ and $ND_2$ at $B = 5$ T, $r_N/r_E < 10^{-2}$ for both electronic states.

Once the temperature and field strength are fixed, there is no experimental control over $r_E$, $r_{N,gnd}$, and $r_{N,exc}$, but there is control of $k_E$ and $k_N$. Consideration of the EPR transition probability $k_E$ starts with the following expression for purely monochromatic microwave radiation:

$$k_E(\omega_{\mu w}) = (\mu_B B_{\mu w})^2 g(\omega_{\mu w} - \omega_c)\hbar^2 = 7.73\times 10^{21} B_{\mu w}^2 g(\omega_{\mu w} - \omega_c) \ \ (\mathrm{T\,s})^{-2}, \tag{11}$$

where $\mu_B$ is the Bohr magneton, $g(\omega_{\mu w} - \omega_c)$ the normalized EPR spin-packet line shape function, and $\omega_c$ the center frequency. While there are formulas relating $B_{\mu w}^2$ to incident microwave power, resonant cavity dimensions, and $Q$, it is more reliable to measure $B_{\mu w}^2$ directly by the method of perturbing spheres [17], especially when the cavity encloses a Dewar tail and/or other apparatus of significant volume. $B_{\mu w}$ will normally be $10^{-5}$ T or less. With the definition

$$\Delta\omega_{sp} \equiv \text{half-width of the spin-packet function}$$

and the relation $\int g(\omega - \omega_c) d\omega = 1$, the average value of the spin-packet function is estimated to be

$$\langle g(\omega_{\mu w} - \omega_c)\rangle 0.5/\Delta\omega_{sp}. \tag{12}$$

The energy difference $E_c - E_a$ is lifetime broadened by the processes, acting in parallel, which populate and deplete the two states involved. The lifetime $\tau$ and $\Delta\omega_{sp}$ expressed in terms of rates defined above (where constants of the order of 1, e.g., $1 - \lambda^2$, multiplying them are omitted) are

$$\Delta\omega_{sp} = 1/\tau \approx k_E + k_N + r_E + r_N. \tag{13}$$

Results of simulations, described below with examples in Fig. 2, show that proton polarization comes close to its limiting value when $k_E \approx 10^4\ s^{-1}$ and $k_N \approx 10^3\ s^{-1}$. It follows from Eq. (13) that $\Delta\omega_{sp} \approx k_E \approx 10^4\ s^{-1}$. Because this width is comparable with the spectral purity (bandwidth) of the radiation of microwave sources in general use (see, e.g., [18]), the microwave radiation is spread out over the spin packet and

$$k_E = \langle k_E(\omega_{\mu w})\rangle = 7.73\times 10^{21} B_{\mu w}^2 \langle g(\omega_{\mu w} - \omega_c)\rangle (\mathrm{T\,s})^{-2} = 7.73\times 10^{21} B_{\mu w}^2 (0.5/\Delta\omega_{sp}) \ \ (\mathrm{T\,s})^{-2} \tag{14}$$

or

$$B_{\mu w}^2 = 2.6\times 10^{-22} k_E \Delta\omega_{sp} \ \ (\mathrm{T\,s})^2. \tag{15}$$

There is no problem in generating microwave fields that produce $k_E$'s as fast as $10^4\ s^{-1}$; to $\Delta\omega_{sp} \approx k_E \approx 10^4\ s^{-1}$ corresponds $B_{\mu w}^2 \approx 2.6\times 10^{-14}\ T^2$ or $(1.6\times 10^{-3}\ G)^2$. In experimental terms, a microwave magnetic field of $(B_{\mu w,max})^2 = 3\times 10^{-10}\ T^2$ can be generated with 0.12 $\mu$W of power entering a 22.5 GHz ("$K$ band," 0.8 T for free radical resonance) good quality, full wavelength cavity. The power needed decreases with decreasing cavity volume, and cavity volume per wavelength decreases with increasing microwave frequency; e.g., $(B_{\mu w,max})^2 = 3\times 10^{-10}\ T^2$ requires $\approx 0.05$ $\mu$W in a full wavelength cavity at 35 GHz ("$Q$ band," 1.25 T). Greater powers are required when larger sample volumes (more wavelengths) are needed. In very successful experiments on electron scattering from DNP polarized protons or deuterons in a 5 T constant magnetic field, the target material is not in a resonant cavity [6]; direct and intense 140GHz microwave radiation is employed to excite one forbidden EPR transition or the other. The same configuration could be used to excite allowed transitions in the ENDOR-DNP method proposed here, but much less power would be needed.

There is also no problem with spectral resolution—being able to excite one transition (e.g., $a$ to $c$) with only negligible microwave power within a spin packet of the other ($b$ to $d$). For example, to $\Delta\omega_{sp} = 10^4\ s^{-1}$ corresponds an energy less than $10^{-6}\ cm^{-1}$, more than 100 times smaller than the smallest hyperfine splitting in the $NH_2$ radical [10]. Anisot-

ropy in the hyperfine splitting or the electronic $g$ tensor is likely to have a greater effect upon spectral resolution than does spin-packet width.

Consideration of $k_N$ is similar to that of $k_E$ except for two quantitative differences. First, because nuclear magnetic dipoles are $\approx 10^3$ times smaller than electronic magnetic dipoles, the production of NMR transition rates comparable with EPR rates requires NMR rf fields much greater than EPR microwave fields. Further, there are substantial differences among nuclei; e.g., the proton, with spin $I_P=1/2$, has nuclear $g$ value 5.5857 and the deuteron, with spin $I_D=1$, has nuclear $g$ value 0.857 44. Also, the bandwidths of rf sources are generally narrower than those of microwave sources; it suffices to take $g(\omega_{rf}-\omega_c)$ at its center. [Here $g(\omega_{rf}-\omega_c)$ is the normalized NMR spin-packet line shape function with $\omega_c$ the central NMR frequency.] Choosing again the allowed EPR transition to be between $a$ and $c$, one sees that the relevant NMR transition is between $c$ and $d$. It follows that, through state $c$, the major source of line broadening of the NMR energy difference $E_d-E_c$ is the same as that of the EPR difference $E_c-E_a$, and the same spin packet width $\Delta\omega_{sp}\approx k_E$ applies to the NMR transition. For nucleus $j$ of spin $I_j$ and $g$ value $g_j$,

$$k_N=\sigma^2(g_j\mu_n B_{rf})^2/(\Delta\omega_{sp}\hbar^2), \tag{16}$$

where $\sigma^2=1$ for $I_j=1/2$, 2 for $I_j=1$, etc., as required by $I_\pm$; $\mu_n$ is the nuclear magneton, and $g(\omega_{rf}-\omega_c=0)=1/\Delta\omega_{sp}$. It follows that

$$k_N(\text{proton})=7.16\times 10^{16}(B_{rf}^2/\Delta\omega_{sp})(\text{T s})^{-2} \tag{17a}$$

and

$$B_{rf}^2(\text{proton})=1.40\times 10^{-17}k_E k_N(\text{T s})^2. \tag{17b}$$

To reach close to maximum polarization, $k_E\approx 10^4\ \text{s}^{-1}$ and $k_N\approx 10^3\ \text{s}^{-1}$, in which case $B_{rf}^2(\text{proton})\approx 1.40\times 10^{-10}\ \text{T}^2$ or $(0.12\ \text{G})^2$. ENDOR spectrometer technology effectively deals with the small skin depths at NMR frequencies, depths which severely reduce cavity wall penetration by rf magnetic fields. In one example, rf fields of 6 G peak to peak have been produced by coils secured to the outside of $X$-band cavity walls [19,20].

For the deuteron

$$k_N(\text{deuteron})=1.69\times 10^{15}(B_{rf}^2/\Delta\omega_{sp})(\text{T s})^{-2} \tag{18a}$$

$$\text{and } B_{rf}^2(\text{deuteron})=5.92\times 10^{-16}k_N k_E(\text{T s})^2. \tag{18b}$$

## V. STEADY STATE AND KINETICS

Upon setting $df_a/dt=df_b/dt=df_c/dt=0$ in Eqs. (1)–(3) for nuclear spin 1/2, one arrives at a set of three algebraic equations, the solution of which gives the steady-state values of $f_a$, $f_b$, and $f_c$ as functions of the rate parameters, the overlap, and $f_{a,eq}$, $f_{b,eq}$, $f_{c,eq}$, and $f_{d,eq}$. Because the latter thermal equilibrium values depend strongly upon both the temperature and magnetic field strength, so do the steady-state values of the four fractional populations. With the steady-state values, one immediately obtains $f_{d,ss}=1-f_{a,ss}-f_{b,ss}-f_{c,ss}$. The fractional polarization (continuing with nuclear spin down) is

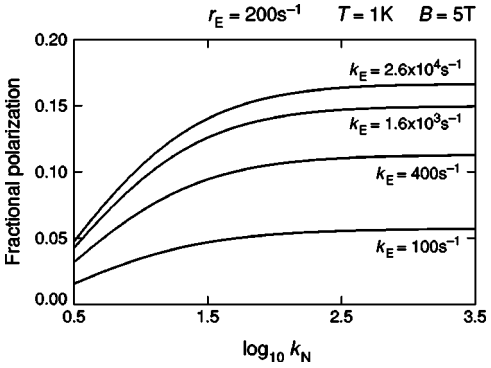


FIG. 3. Polarization of a deuteron in $ND_2$ as a function of $k_N$ for several values of $k_E$ when $r_E=200\ \text{s}^{-1}$. $T=1$ K and $B=5$ T.

$$p=-(f_{b,ss}+f_{d,ss}-f_{a,ss}-f_{c,ss}). \tag{19}$$

In the examples given below, the hyperfine energies of the ground and excited electronic levels are taken to be those of $NH_2$ [10]. For $T=1$ K and $B=5$ T, Fig. 2 shows $p$ as a function of $k_N$ for several values of $k_E$ when $r_E=1\ \text{s}^{-1}$ (a), $200\ \text{s}^{-1}$ (b) and $1000\ \text{s}^{-1}$ (c); $r_N$ is calculated from Eq. (10a) with $|H_{mix}|^2$ averaged over $\psi$ at $\theta=60°$ as in Fig. 1 of [10]. The maximum attainable $p$ is seen to be 1/2 at $T=1$ K and $B=5$ T, at which $T$ and $B$, $f_{a,eq}\approx f_{b,eq}\approx 0.5$ and $f_{c,eq}\approx f_{d,eq}\approx 0.0$. Also, at $B=5$ T, $\lambda^2\approx 0$. The fraction 1/2 is readily arrived at by considering the steady-state equations when $k_E, k_N \gg r_E \gg r_{N,gnd}$. With $df_a/dt=0$, $k_E \gg r_E, r_N$ in Eq. (1) requires $f_a\approx f_c$. With $df_c/dt=0$ and $f_a\approx f_c$, $k_N \gg r_E, r_N$ in Eq. (3) requires $f_d\approx f_c$. With $df_b/dt=0$, $r_E \gg r_{Ngnd}$ in Eq. (2) requires $f_b-f_d\approx f_{b,eq}-f_{d,eq}\approx 0.5$, given $T=1$ K, $B=5$ T. Under these conditions, the population of state $a$ undergoes a major decrease while that of $b$ increases somewhat; significant populations appear in states $c$ and $d$ but their nuclear spins are equal and opposite. Had the allowed EPR transition $b$ to $d$ been chosen together with the $d$ to $c$ NMR transition, there would be a limiting positive polarization of 1/2. Whether up or down nuclear polarization is sought, in the steady state essentially half of the equilibrium electron spin polarization can be transferred to the nuclear spins.

By means analogous to those used above for the proton, one predicts that fractional spin polarization of a deuteron in $ND_2$ as great as 1/6 can be produced by ENDOR-DNP The steady-state fractional polarization associated with Eqs. (5)–(9) is

$$\text{net polarization}=-(f_{c,ss}+f_{f,ss}-f_{a,ss}-f_{d,ss}) \tag{20}$$

and is shown in Fig. 3 as a function of $k_N$ for several values of $k_E$ when $r_E=200\ \text{s}^{-1}$.

Formulation of the time course of polarization is simplified with little effect upon all but the end of the kinetic

curves by neglecting the much slower $r_N$ terms and then rewriting the differential equations in terms of difference populations $x$, $y$, and $z$:

$$x \equiv f_d - f_a, \quad y \equiv f_d - f_c, \quad \text{and} \quad z \equiv f_c - f_b. \tag{21}$$

$dx/dt$, $dy/dt$, and $dz/dt$ are readily expressed in terms of $x$, $y$, and $z$ from the original rate equations (1)–(3). The algebraic path then chosen was to express $y$, $dy/dt$, $x$, and $dx/dt$ as functions of $z$, $dz/dt$, $d^2z/dt^2$, and $d^3z/dt^3$. One then arrives at the following third order linear differential equation for $z$:

$$d^3z/dt^3 + 2(k_E + k_N + 2r_E)d^2z/dt^2 + [4rE(k_E + r_E) + 3k_N(k_E + 2r_E)]dz/dt + 4k_N(k_E + r_E)r_E(z + f_{b,ss} - f_{c,ss}) = 0 \tag{22}$$

to which belongs the auxiliary equation

$$r^3 + 2(k_E + k_N + 2r_E)r^2 + [4r_E(k_E + r_E) + 3k_N(k_E + 2r_E)]r + 4k_N(k_E + r_E)r_E = 0. \tag{23}$$

Exact solutions show that, under the conditions $k_E \geqslant k_N > r_E$, the roots of Eq. (22) are, to a very good approximation,

$$r_{1,2} = -k_E + k_N + \alpha r_E \pm [k_E^2 - k_E k_N + k_N^2 + r_E(k_N + r_E)]^{1/2}$$

and

$$r_3 = -8k_N r_E/3(2k_N + r_E), \tag{24}$$

where $\alpha \equiv 2(4k_N + 3r_E)/3(2k_N + r_E)$.

The solution for $z$ is

$$z(t) = A\ \exp(r_1 t) + B\ \exp(r_2 t) + C\ \exp(r_3 t) + Dt + E. \tag{25}$$

$t \to \infty$ corresponds to the steady state, which shows that $D = 0$ [from both $z(\infty)$ being finite and $dz/dt(\infty) = 0$] and

$$E = z(\infty) = f_{c,ss} - f_{b,ss}. \tag{26}$$

From Eqs. (21), (25), and (26), $z(0) = A + B + C + E = f_{c,eq} - f_{b,eq}$ or

$$A + B + C = f_{c,eq} - f_{b,eq} - (f_{c,ss} - f_{b,ss}). \tag{27}$$

Proceeding in a similar manner with $dz/dt$ and $d^2z/dt^2$ at $t = 0$, one finds

$$r_1 A + r_2 B + r_3 C = k_N(f_{d,eq} - f_{c,eq}) \tag{28}$$

and

$$r_1^2 A + r_2^2 B + r_3^2 C = -k_E k_N(f_{d,eq} - f_{a,eq}) - 2k_N^2(f_{d,eq} - f_{c,eq}) - 2k_N r_E(f_{d,eq} - f_{c,eq}). \tag{29}$$

After solving the three equations (27)–(29) for $A$, $B$, and $C$, one obtains $z(t)$ and its derivatives, and then $x(t)$ and $y(t)$. The fractional populations at arbitrary time follow from writing them in terms of $x$, $y$, and $z$. Note that, because the small $r_N$ terms are not included in this kinetic analysis, and $z(\infty)$ is the only difference population from the steady-state results which is used as a boundary condition, the values of $f_a(\infty)$, $f_b(\infty)$, $f_c(\infty)$, and $f_d(\infty)$ will be slightly different from those obtained from the steady-state formulation (as in the example presented in the next paragraph).

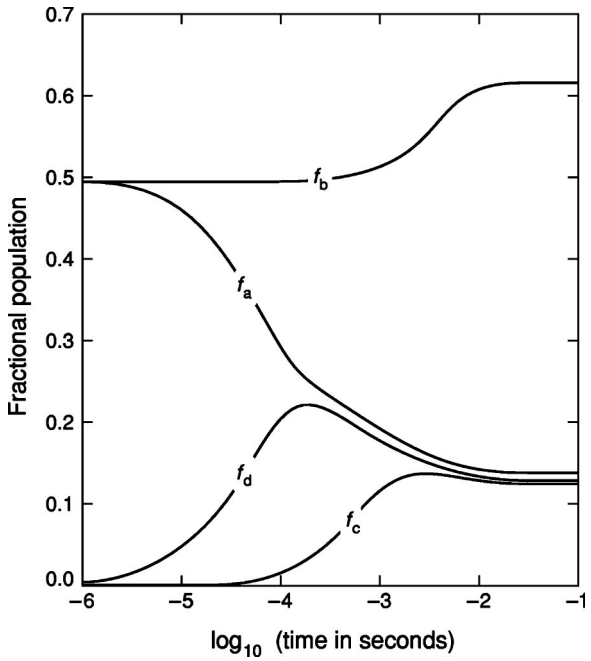


FIG. 4. Time courses of the populations of the four hyperfine states of a proton in $NH_2$. The rate constants are $k_E = 1.0 \times 10^4\ s^{-1}$, $k_N = 1.0 \times 10^3\ s^{-1}$, and $r_E = 200\ s^{-1}$. $T = 1$ K and $B = 5$ T.

Figure 4 shows the time courses of the populations of the four states of a proton in $NH_2$ when $r_E = 200\ s^{-1}$ [as in Fig. 2(b)] with $k_E(10^4\ s^{-1})$ and $k_N(10^3\ s^{-1})$ chosen to result in a steady-state polarization close to the limiting value of 1/2. For this case, the values of $f_a(\infty)$ from the kinetic and state formulations differ by 0.66%, those of $f_b(\infty)$ by 0.19%, those of $f_c(\infty)$ by 0.96%, and those of $f_d(\infty)$ by 1.19%.

## VI. DISCUSSION

Formulation of ENDOR-mediated DNP, for an ideal system, and simulations based upon this formulation are reported above. (Real systems can differ from the ideal one; there can be several paramagnetic nuclei, not necessarily of the same kind or in the same electronic environment, and the electron spin can be delocalized into orbitals of several atoms.) The proposed method is computationally demonstrated to have the potential for producing useful nuclear polarization, approaching 50% for spin 1/2, quickly and with low microwave power. Considerations that have arisen in the course of this research, together with the results, call for future research.

(1) Knowledge of electron spin-lattice relaxation times is essential for quantification of the kinetics of any DNP method, and the required measurements have not yet been

carried out under appropriate conditions of very low temperatures and very high magnetic field strengths.

(2) In order to realize the potential of the proposed method, instrumentation with this low $T$ and high $B$ capability needs to be modified to accommodate precisely controlled (with regard to both frequency and power) microwave and radiofrequency fields, and simultaneous measurement of intramolecular nuclear polarization; (properties of the system to be polarized may impose specific instrumentation requirements).

(3) Because bulk polarization is useful in many applications, once the ENDOR-DNP method is functioning, spin diffusion from polarized intramolecular sites requires investigation.

While reduced from values possible at the 1 K and 5 T conditions employed above, considerable polarizations can be obtained by ENDOR-DNP at higher temperatures and weaker fields. For example, at $T=4.2$ K and $B=1$ T, the proton polarization in $NH_2$ would be 2.4% for $r_E=840\ s^{-1}$ (taken 4.2 times faster than at 1 K) with, as above, $k_E=1.0\times10^4\ s^{-1}$ and $k_N=1.0\times10^3\ s^{-1}$. If, at this $T$ and $B$, the microwave and rf powers were both increased by a factor of ten, the polarization would be 5.2%. These polarizations, which can be up or down, are 100 and just over 200 times greater than the polarization (up) of free protons at 4.2 K and 1 T, the static value being 0.0243%. Corresponding increases over the static method are predicted for deuteron polarization by ENDOR-DNP.

## ACKNOWLEDGMENTS

I thank D. G. Crabb and O. Rondon-Aramayo for helpful comments on the manuscript. This research was supported by the Academic Enhancement Program of the University of Virginia.

[1] G. J. Gerfen, L. R. Becerra, D. A. Hall, R. G. Griffen, R. J. Temkin, and D. J. Singel, J. Chem. Phys. **102**, 9494 (1995).
[2] M. S. Albert, G. D. Cates, B. Driehuys, W. Happer, B. Saam, C. S. Springer, Jr., and A. Wishnia, Nature (London) **370**, 199 (1994).
[3] G. Navon, Y.-Q. Song, T. Rõõm, S. Appely, R. E. Taylor, and A. Pines, Science **271**, 1848 (1996).
[4] R. M. Kulsrud, H. P. Furth, E. J. Valeo, and M. Goldhaber, Phys. Rev. Lett. **49**, 1248 (1982).
[5] A. Abragam and J. Krisch, in *Hyperfine Interactions*, edited by A. J. Freeman and R. B. Frankel (Academic, New York, 1967), Chap. 8.
[6] T. D. Averett, D. G. Crabb, D. B. Day, T. J. Liu, J. S. McCarthy, J. Mitchell, O. Rondon, D. Zimmermann, I. Sick, B. Zihlmann, G. Court, H. Dutz, W. Meyer, A. Rijllart, S. St. Lorant, J. Button-Shafer, and J. Johnson, Nucl. Instrum. Methods Phys. Res. A **427**, 440 (1999).
[7] W. Knop, M. Hirai, G. Olah, W. Meerwinck, H.-J. Schink, H. B. Stuhrman, R. Wagner, M. Wenkow-EsSouni, J. Zhao, O. Scharpf, R. R. Crichton, M. Krumpole, K. H. Nierhaus, T. O. Niinikoski, and A. Rijllart, Physica B **174**, 275 (1991).
[8] T. Guiberteau and D. Grucker, J. Magn. Reson., Ser. A **110**, 47 (1996).
[9] G. Feher, Phys. Rev. **114**, 1219 (1959).
[10] A. R. Airne and A. S. Brill, Phys. Rev. A **63**, 052511 (2001).
[11] T. E. Gunter and C. D. Jeffries, Phys. Rev. **159**, 290 (1967).
[12] V. Bouffard, T. Roinel, P. Robineau, and A. Abragam, J. Phys. (France) **41**, 1447 (1980).
[13] J. Michalik and L. Kevan, J. Chem. Phys. **68**, 5325 (1978).
[14] S. S. Eaton, J. Harbridge, G. A. Rinard, G. R. Eaton, and R. T. Weber, Appl. Magn. Reson. **20**, 151 (2001).
[15] C. T. Farrar, D. A. Hall, G. J. Gerfen, S. J. Inati, and R. G. Griffen, J. Chem. Phys. **114**, 4922 (2001).
[16] A. Abragam, *The Principles of Nuclear Magnetism* (Clarendon Press, Oxford, 1955), p. 380.
[17] F. G. Fiamingo, A. S. Brill, D. A. Hampton, and R. Thorkildsen, Biophys. J. **55**, 67 (1989).
[18] A. S. Brill, C.-I. Shyr, and T. C. Walker, Mol. Phys. **29**, 437 (1975).
[19] H. L. Van Camp, C. P. Scholes, and R. A. Isaacson, Rev. Sci. Instrum. **47**, 516 (1976).
[20] C. P. Scholes, A. Lapidot, R. Mascarenhas, T. Inubushi, R. A. Isaacson, and G. Feher, J. Am. Chem. Soc. **104**, 2724 (1982).